

CHAPTER 8

Radiative Forcing and Temperature Trends

Lead Author:

K.P. Shine

Co-authors:

K. Labitzke

V. Ramaswamy

P.C. Simon

S. Solomon

W.-C. Wang

Contributors:

C. Brühl

J. Christy

C. Granier

A.S. Grossman

J.E. Hansen

D. Hauglustaine

H. Mao

A.J. Miller

S. Pinnock

M.D. Schwarzkopf

R. Van Dorland

CHAPTER 8

RADIATIVE FORCING AND TEMPERATURE TRENDS

Contents

SCIENTIFIC SUMMARY	8.1
8.1 INTRODUCTION	8.3
8.2 RADIATIVE FORCING DUE TO OZONE CHANGE	8.3
8.2.1 Recent Calculations	8.3
8.2.1.1 Stratospheric Ozone Change	8.3
8.2.1.2 Tropospheric Ozone Change	8.4
8.2.1.3 Net Effect of Ozone Change	8.5
8.2.2 Intercomparison of Models Used to Calculate Radiative Forcing	8.5
8.2.3 General Circulation Model Calculations	8.9
8.2.4 Attribution of Ozone Radiative Forcing to Particular Halocarbons	8.10
8.2.5 Outstanding Issues	8.11
8.3 OBSERVED TEMPERATURE CHANGES	8.12
8.3.1 Effects of the Volcanic Eruptions, Especially Mt. Pinatubo	8.12
8.3.2 Long-Term Trends	8.13
8.3.3 Interpretation of Trends	8.17
8.4 HALOCARBON RADIATIVE FORCING	8.18
8.4.1 Comparison of IR Absorption Cross Sections	8.18
8.4.2 Comparison of Radiative Forcing Calculations	8.20
REFERENCES	8.23

SCIENTIFIC SUMMARY

I. Radiative Forcing and Climatic Impact of Ozone Change

- Recent one-dimensional studies support earlier conclusions that between 1980 and 1990 the observed decrease in stratospheric ozone has caused a negative global-mean radiative forcing (*i.e.*, it acts to cool the climate) that is about -0.1 Wm^{-2} ; this can be compared to the direct radiative forcing due to changes in CO_2 , CH_4 , N_2O , and the chlorofluorocarbons (the “well-mixed” gases) of about 0.45 Wm^{-2} over the same period. An accurate assessment of the potential climatic effect of changes in stratospheric ozone is limited by the lack of detailed information on the ozone change, especially in the vicinity of the tropopause. A limited sensitivity study using different assumptions about the vertical profile of ozone loss indicates that, for the same change in total column ozone, the ozone forcing could conceivably be up to a factor of two less negative.
- Model simulations and deductions from limited observations of the increase in tropospheric ozone since pre-industrial times suggest a positive global-mean forcing that may be around 0.5 Wm^{-2} ; this can be compared to the direct radiative forcing due to changes in well-mixed gases of about 2.4 Wm^{-2} over the same period. Particular difficulties are the verification of the geographical extent of the tropospheric ozone increases and the problems in accurately specifying the vertical profile of the change.
- On the basis of these estimates, the net global-mean radiative forcing due to ozone changes is likely to have been positive since pre-industrial times. However, Chapter 1 indicates that tropospheric ozone has changed little since 1980 and so, since then, the stratospheric ozone change is likely to have dominated, giving a negative global-mean forcing due to ozone changes.
- An intercomparison of radiation codes used in assessments of the radiative forcing due to ozone changes has shown that, in general, differences between these codes can be explained; the intercomparison highlights the detail with which solar and thermal infrared processes must be represented.
- The only general circulation model (GCM) experiment to investigate the climatic impact of observed lower stratospheric ozone loss between 1970 and 1990 indicates the expected surface cooling in response to the negative radiative forcing.
- Other GCM simulations raise important, but as yet unresolved, issues about the way in which the global mean of a spatially very inhomogeneous radiative forcing, such as that due to ozone change, can be directly compared to the global-mean forcing due to, for example, changes in well-mixed greenhouse gases.
- The previous assessment noted that the negative radiative forcing due to stratospheric ozone loss in the 1980s is of a similar size as, but the opposite sign to, the positive direct radiative forcing due to halocarbons over the same period. Attempts have been made to partition the indirect negative forcing due to ozone loss amongst individual halocarbons. They have emphasized that bromocarbons are, on a per molecule basis, much more efficient at destroying ozone than chlorofluorocarbons (CFCs). One evaluation attributes about 50% of the 1980-1990 negative forcing to the CFCs; since the CFCs dominate the direct forcing, their net effect is reduced by about 50% due to the ozone loss. Carbon tetrachloride and methyl chloroform each contribute about 20%, while bromocarbons contribute about 10% to the indirect forcing; these species contribute relatively little to the direct forcing so their net effect is likely to be negative.

RADIATIVE FORCING

II. Lower Stratospheric Temperature Trends

- The temperature of the lower stratosphere showed a marked rise, of about 1 deg C in the global mean, due to the radiative effects of increases in stratospheric aerosol loading following the eruption of Mt. Pinatubo in June 1991. The maximum warming occurred in the six months following the eruption; temperatures have now returned to near pre-eruption levels. This warming has been successfully simulated by GCMs.
- Data from radiosondes over the past three decades and satellite observations since the late 1970s continue to support the existence of a long-term global-mean cooling of the lower stratosphere of about 0.25 to 0.4 deg C/decade; there is some indication of an acceleration in this cooling during the 1980s, but the presence of large temperature perturbations induced by volcanic aerosols makes trend analysis difficult.
- Model calculations indicate that ozone depletion is likely to have been the dominant contributor to the temperature trend in the lower stratosphere since 1980 and is much more important than the contribution of well-mixed greenhouse gases. In addition, observed temperature trends since 1979 are found to be significantly negative at the same latitudes and times of year as significant decreases in column ozone, with the exception of the southern midlatitudes in midwinter. However, there are other potential causes of lower stratospheric temperature change (such as changes in stratospheric water vapor or cirrus clouds) whose contributions are difficult to quantify.

III. Radiative Properties of Halocarbon Substitutes

- More laboratory measurements of the infrared absorption cross sections of actual and proposed substitutes to chlorofluorocarbons have become available, including molecules not hitherto reported in assessments. These cross sections have been included in radiative transfer models to provide estimates of the radiative forcing per molecule. The radiative forcing estimates are subjectively estimated to be accurate to within 25%, but not all of the studies have yet been reported in adequate detail in the open literature; this hinders a detailed understanding of differences in existing estimates.

8.1 INTRODUCTION

In recent ozone assessments, changes in the radiation balance have been an issue because (i) the chlorofluorocarbons (CFCs) and their hydrohalocarbon replacements are powerful absorbers of infrared radiation and (ii) changes in stratospheric ozone have been shown to cause a significant radiative forcing of the surface-troposphere system (WMO, 1992). Hence both factors are of potential importance in understanding climate change.

The aim of this Chapter is to provide an update of research in these two areas. In addition, significant changes in stratospheric temperature have been reported in recent assessments (WMO, 1988); it is believed that changes in the radiative properties of the stratosphere are an important part of the cause of the temperature trends. Changes in ozone appear to be of particular significance; in turn, ozone may itself be affected by the temperature changes. This Chapter will update both the observations of temperature changes and our understanding of their causes; we will concentrate on the lower stratosphere because ozone losses are believed to be greatest in this region and also because it is changes in this region that are believed to be of most climatic significance.

It is not our aim to provide an overall assessment of our understanding of the radiative forcing of climate change. Such an assessment will be part of IPCC (1994). Instead we concentrate on the radiative forcing due to halocarbons and ozone change, building on the discussion in IPCC (1994). In common with the rest of this assessment, we will also consider the role of tropospheric ozone changes.

One important discussion in IPCC (1994) concerns the utility of the entire concept of radiative forcing. Radiative forcing is defined as the global-mean change in the net irradiance at the tropopause following a change in the radiative properties of the atmosphere or in the solar energy received from the Sun. As discussed in IPCC (1994), the preferred definition includes the concept of stratospheric adjustment, in which the stratospheric temperatures are allowed to alter such as to re-establish a state of global-mean radiative equilibrium; this process is of particular relevance when considering the forcing due to stratospheric ozone change.

The utility of radiative forcing has been based on model results indicating that the climate response is es-

entially independent of the forcing mechanism. Thus, a radiative forcing of $x \text{ Wm}^{-2}$ due to a change in greenhouse gas concentration would give essentially the same climate response as $x \text{ Wm}^{-2}$ at the tropopause due to, say, a change in solar output; this is despite the fact that the two mechanisms involve rather different partitioning of the irradiance change between the surface and troposphere as well as between different latitudes and seasons.

Recent, and rather preliminary, results from general circulation models (GCMs) indicate that this relationship may not be so well-behaved for radiative forcings due to changes in ozone and tropospheric aerosols, where there are strong vertical, horizontal, and temporal variations in both the concentrations of the species and their changes with time.

If this work were to be confirmed, it would make it more difficult to intercompare the forcings in Wm^{-2} between different climate change mechanisms; in particular it might be difficult to add the forcings from different mechanisms to achieve a meaningful total forcing.

Hence radiative forcing must be used with some caution, although much more work is needed to investigate whether the concept lacks general validity. Radiative forcing remains a useful measure for intercomparing different calculations of ozone forcing and for intercomparing the strength of different halocarbons.

8.2 RADIATIVE FORCING DUE TO OZONE CHANGE

8.2.1 Recent Calculations

8.2.1.1 STRATOSPHERIC OZONE CHANGE

The principal features outlined in IPCC (1992) and WMO (1992) concerning the net radiative forcing of the surface-troposphere system due to ozone depletion in the lower stratosphere are:

- a) the distinction between the solar component that acts to heat the surface-troposphere system and the longwave component that tends to cool it;
- b) the difference between the instantaneous forcing (referred to as "Mode A" in WMO, 1992)

RADIATIVE FORCING

and the forcing calculated using adjusted stratospheric temperatures (referred to as “Mode B” in WMO, 1992); the consequent cooling of the lower stratosphere enhances the longwave radiative effects to give a net negative forcing.

These features have been supported by several model studies (Ramaswamy *et al.*, 1992; Wang *et al.*, 1993; Shine, 1993; Karol and Frolikis, 1994), as well as by an intercomparison exercise to be discussed in Section 8.2.2.

An accurate knowledge of the magnitude of the ozone loss in the lower stratosphere in different regions is crucial in evaluating the global-mean radiative forcing. Chapter 1 indicates the possibility of a small ozone depletion in the tropics. The radiative forcing consequences of such a loss would depend on the vertical profile of the loss profile; it could be significant if it were to be concentrated in the lower stratosphere (Schwarzkopf and Ramaswamy, 1993).

The radiative forcing is strongly governed by the shape of the vertical profile of the ozone loss, particularly in the vicinity of the tropopause (Wang *et al.*, 1980; Lacis *et al.*, 1990). While it is unambiguously clear that a loss of ozone in the lower stratosphere will lead to a negative radiative forcing of the surface-troposphere system, the precise value is dependent on the assumed altitude shape of the ozone change.

Schwarzkopf and Ramaswamy (1993) examine this problem by using 1978-1990 ozone changes at altitudes above 17 km derived from Stratospheric Aerosol and Gas Experiment (SAGE) observations; they make a range of assumptions about how the ozone changes between the tropopause and 17 km. The results can be quoted in terms of the radiative forcing per Dobson unit (DU) change in stratospheric ozone. Their results depend on latitude, mainly because a smaller fraction of the ozone depletion is located near the tropopause at higher latitudes. In the tropics, the estimates range from 0.007 to 0.01 Wm^{-2}/DU ; at midlatitudes the relative uncertainty is greater with a range of 0.003 to 0.008 Wm^{-2}/DU . Such values are obviously dependent on the SAGE ozone change profiles used in the calculations.

Wang *et al.* (1993) report instances where the change in stratospheric ozone results in a warming rather than a cooling of the surface-troposphere system; this can be explained by the fact that the position of the tropopause in these calculations is such that some of the

ozonesonde-observed increases in tropospheric ozone are attributed to the lower stratosphere. Hauglustaine *et al.* (1994) also find that the decrease in stratospheric ozone causes a warming of the surface-troposphere system. They used a 2-D chemical-dynamical-radiative model to simulate changes in concentration of a number of gases, including ozone, since pre-industrial times; the sign of the stratospheric ozone effect in their model appears to be because, in the Northern Hemisphere at least, their model simulates less ozone depletion in the lower stratosphere than is indicated by recent observations – their fractional ozone loss is found to be highest in the mid- to upper stratosphere, where a decrease in ozone leads to a positive radiative forcing (Lacis *et al.*, 1990). The model of Hauglustaine *et al.* (1994) does include an interactive dynamical response, so they are not dependent on assumptions such as those required when applying fixed dynamical heating.

These recent model studies highlight the need for a detailed consideration to be given to the vertical profile of the depletion and for consistency between the tropopause level chosen to estimate the surface-troposphere forcing and the altitude profile of the ozone change. Model-dependent factors are also significant for the accuracy of the computed forcing, as will be discussed in Section 8.2.2.

The overall effect of observed stratospheric ozone depletion on radiative forcing has not been significantly updated since WMO (1992), which reported a forcing of about -0.1 Wm^{-2} between 1980 and 1990. Hansen *et al.* (1993) compute a global mean change of $-0.2 \pm 0.1 \text{ Wm}^{-2}$ between 1970 and 1990. Such values represent a small but not negligible offset to the greenhouse forcing from changes in CO_2 , CH_4 , N_2O , and CFCs (the so-called “well-mixed” gases) that result in a forcing of about 0.45 Wm^{-2} between 1980 and 1990. The results of Schwarzkopf and Ramaswamy (1993) show that different assumptions about the vertical profile of ozone change, for the same change in total column ozone, could conceivably result in an ozone forcing up to a factor of two less negative.

8.2.1.2 TROPOSPHERIC OZONE CHANGE

Estimates for the global effect of tropospheric ozone increases are scarcer, mainly because of the difficulties in making global estimates of ozone change from

the limited observations that are available. The model study of Hauglustaine *et al.* (1994) found that their simulated tropospheric ozone increases contributed about 0.5 Wm^{-2} to the radiative forcing; this can be compared to the forcing of about 2.4 Wm^{-2} due to the changes in well-mixed gases since pre-industrial times (IPCC, 1990). (See Chapter 7 for an assessment of the ability of current models to represent tropospheric ozone changes.) Marengo *et al.* (1994) have used observations from France in the late nineteenth century, together with recent observations of the meridional distribution of tropospheric ozone, to make a simple radiative forcing estimate; they derive a global-mean radiative forcing since pre-industrial times of 0.6 Wm^{-2} . Fishman (1991), using observed trends, estimates that between 1965 and 1985, a 1%/year trend in tropospheric ozone applied over the entire Northern Hemisphere implies an approximate global-mean forcing of 0.15 Wm^{-2} , or about 20% of the effect of well-mixed gases over this period. Particular difficulties in all studies of the radiative forcing due to tropospheric ozone change are the verification of the geographical extent of the ozone increases and the problems in accurately specifying the vertical profile of ozone change.

8.2.1.3 NET EFFECT OF OZONE CHANGE

While it is clear that a tropospheric ozone increase would lead to a positive radiative forcing, and that this would be opposite to the effect due to the lower stratospheric losses, the sign of the net effect is uncertain (WMO, 1986; Lacis *et al.*, 1990; Karol and Frolkis, 1994; Schwarzkopf and Ramaswamy, 1993; Wang *et al.*, 1993). Wang *et al.* point out that the net forcing due to the total ozone change in the atmosphere at the locations of the sonde measurements could be positive or negative; at Hohenpeissenberg the net forcing due to ozone changes between the 1970s and 1980s was calculated to be positive and comparable to that due to the increases in the well-mixed greenhouse gases over the same period. Lacis *et al.* (1990), on the other hand, found that for the period 1970-1982, the forcing due to the Hohenpeissenberg changes was negative; however the uncertainty, due to uncertainties in the trend estimate, was large. The effects due to the total atmospheric ozone change are extremely sensitive to the vertical profile of the changes

(both in the troposphere and the stratosphere), the tropopause level assumed, and the latitude and season.

On the basis of these estimates, the net global-mean radiative forcing due to ozone changes is likely to have been positive since pre-industrial times. However, Chapter 1 indicates that tropospheric ozone has changed little since 1980 and so, since then, the stratospheric ozone change is likely to have dominated, giving a negative global-mean forcing due to ozone changes.

8.2.2 Intercomparison of Models Used to Calculate Radiative Forcing

The recent work described above highlights the need to understand the reported differences in radiative forcing due to ozone change. Whilst the overall features of these differences were attributable to different assumptions about the vertical profile of ozone change, it

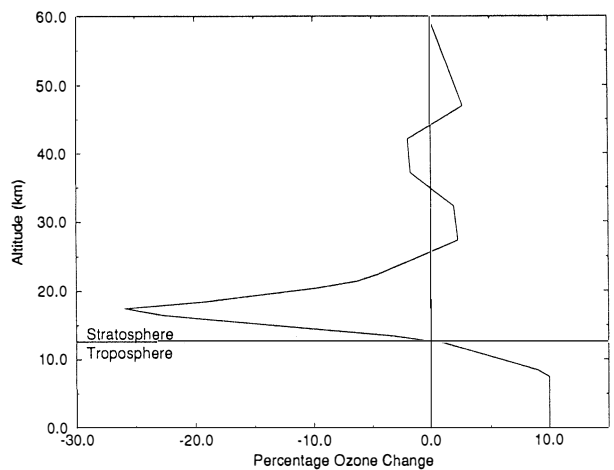


Figure 8-1. Idealized change in ozone as a function of height used solely for the purposes of the intercomparison of radiative codes. The stratospheric change is based on the midlatitude S2 profile of Schwarzkopf and Ramaswamy (1993), which was derived from SAGE/SAGE II measurements during the 1980s above 17 km, then decreasing linearly with altitude to zero at the tropopause at 13 km. The tropospheric increase is an idealized one of 10% up to 8 km, then decreasing linearly with altitude to zero at the tropopause. The stratospheric decrease is 15.5 Dobson units and the tropospheric increase is 3.5 Dobson units. The results shown in Figure 8-2 to 8-4 are calculated using the change in the stratosphere only.

RADIATIVE FORCING

Table 8-1. Participants in Ozone Radiative Forcing Intercomparison and brief description of model type. It is emphasized that the spectral resolution of a radiative transfer scheme is not always a good indication of its accuracy.

Group	Thermal IR scheme	Solar Scheme
GFDL (Geophysical Fluid Dynamics Laboratory)	10 cm ⁻¹ narrow-band code – Ramaswamy <i>et al.</i> (1992)	Wide-band code based on Lacis and Hansen (1974) – two bands in UV and visible
GFDL (2)	Line-by-line code – Schwarzkopf and Fels (1991)	
KNMI (Koninklijk Nederlands Meteorologisch Instituut)	Wide-band scheme amended from Morcrette (1991) to include more trace gases	Wide-band delta-Eddington scheme from Morcrette (1991) – one band in UV and visible
KNMI (2)	As KNMI(1) but including 14 μm band of ozone	As KNMI
LLNL (Lawrence Livermore National Laboratory)	25 cm ⁻¹ narrow-band scheme – Grossman and Grant (1994)	Narrow-band code with 126 bands between 175-725 nm using adding method for scattering – Grossman <i>et al.</i> (1993)
NCAR/CNRS (National Center for Atmospheric Research/ Centre National de la Recherche Scientifique)	Longwave Band Model (LWBM) 100 cm ⁻¹ resolution – Briegleb (1992)	Wide-band scheme based on Lacis and Hansen (1974) – Kiehl <i>et al.</i> (1987)
Reading (University of Reading)	10 cm ⁻¹ narrow-band scheme – Shine (1991)	Delta-Eddington scheme from Slingo and Schrecker (1982) with 10 bands in UV and visible
Reading (2)	As Reading but excluding 14 μm and microwave bands of ozone	As Reading
SUNY (State University of New York)	Wide-band scheme – Wang <i>et al.</i> (1991)	Wide-band scheme based on Lacis and Hansen (1974) – Kiehl <i>et al.</i> (1987)

is important to isolate to what extent differences are due to the radiative transfer methods employed in the studies. An intercomparison of results from different radiative codes was initiated to study this issue. The results are reported in more detail in Shine *et al.* (1994); the main conclusions of the study will be described here.

The intercomparison used tightly specified input parameters to ensure that all groups were using the same conditions. A midlatitude summer clear-sky atmosphere was used with a spectrally constant surface albedo of 0.1. The solar forcing was calculated using an effective daylength and mean solar zenith angle appropriate to 15 April at 45°N. The vertical profile of ozone and ozone

change was specified; the ozone change is shown in Figure 8-1 and is described in the caption. Groups were asked to provide the change in solar and thermal infrared irradiances at the tropopause for both the instantaneous and adjusted forcings (calculated using the fixed dynamical heating assumption [*e.g.*, WMO, 1992]). Three different cases were considered: (i) stratospheric depletion only, (ii) tropospheric increase only, and (iii) both stratospheric depletion and tropospheric increase. The results from the case with stratospheric depletion only will be concentrated on here.

Six groups participated in at least part of the comparison. They are listed in Table 8-1 along with an

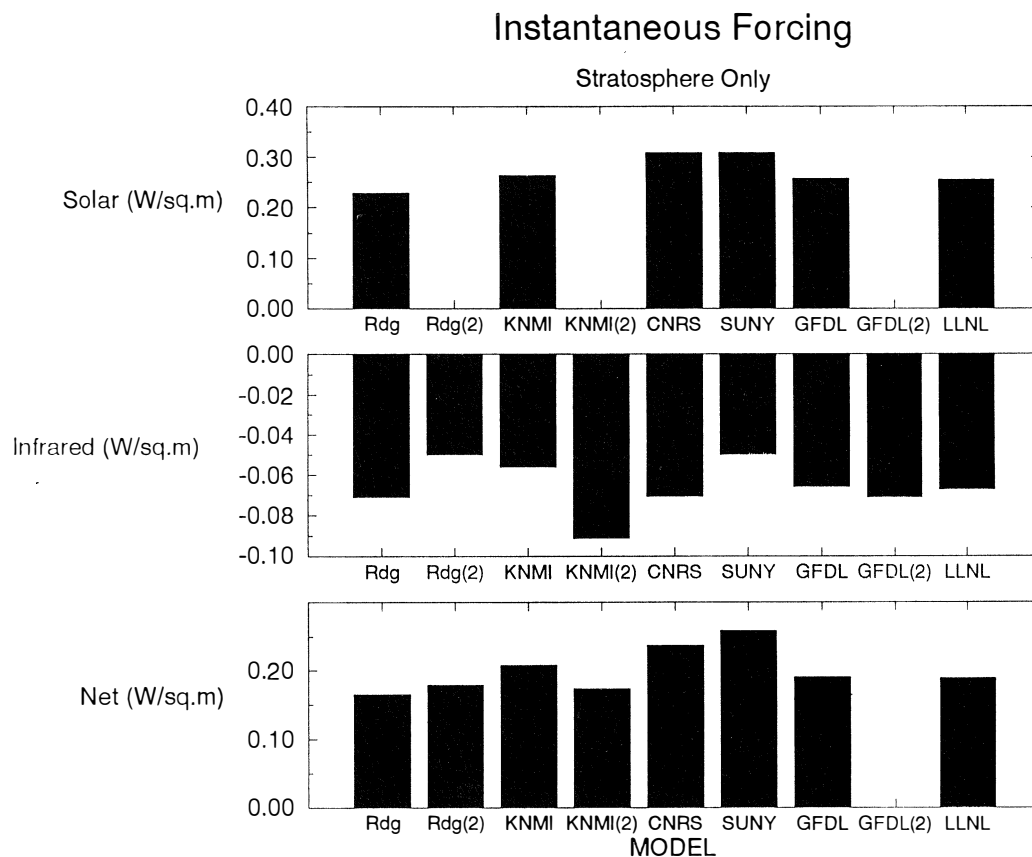


Figure 8-2. Instantaneous changes in solar, thermal infrared, and net (solar minus thermal infrared) irradiances (Wm^{-2}) at the tropopause following a change in ozone in the stratosphere (see Figure 8-1) calculated by the participants in the Ozone Radiative Forcing Intercomparison given in Table 8-1.

indication of the nature of the radiative transfer codes. Some groups contributed results from more than one model configuration.

Figure 8-2 shows the change in solar, thermal infrared, and net irradiance at the tropopause for the instantaneous, stratospheric-depletion case. The spread in solar results is quite marked, ranging from 0.23 to 0.31 Wm^{-2} ; these differences will be discussed later. In all cases the net change is positive, indicating a tendency to warm the surface-troposphere system.

The most important conclusions from the instantaneous case concern the thermal infrared. First, the narrow-band calculations are in very good agreement with the Geophysical Fluid Dynamics Laboratory (GFDL) line-by-line calculations. Second, it became apparent that the results were splitting into two classes – those calculations that included the 14 μm band of ozone

(which is spectroscopically very weak compared to the 9.6 μm band) obtained a forcing of about -0.07 Wm^{-2} , whilst those without this band reported a value of about -0.05 Wm^{-2} ; *i.e.*, the 14 μm band contributes about 30% of the total forcing. The University of Reading calculations were repeated with and without the 14 μm band, and this band was indeed shown to explain the difference. It should be noted that this band is not included in many general circulation model calculations. Further, the 14 μm band contributes only 2% of the change in irradiance for the change in tropospheric ozone only, because in the troposphere this band is more heavily overlapped by pressure-broadened lines of carbon dioxide; this indicates that models that neglect the 14 μm band will give greater relative weight to tropospheric ozone changes compared to stratospheric ozone changes.

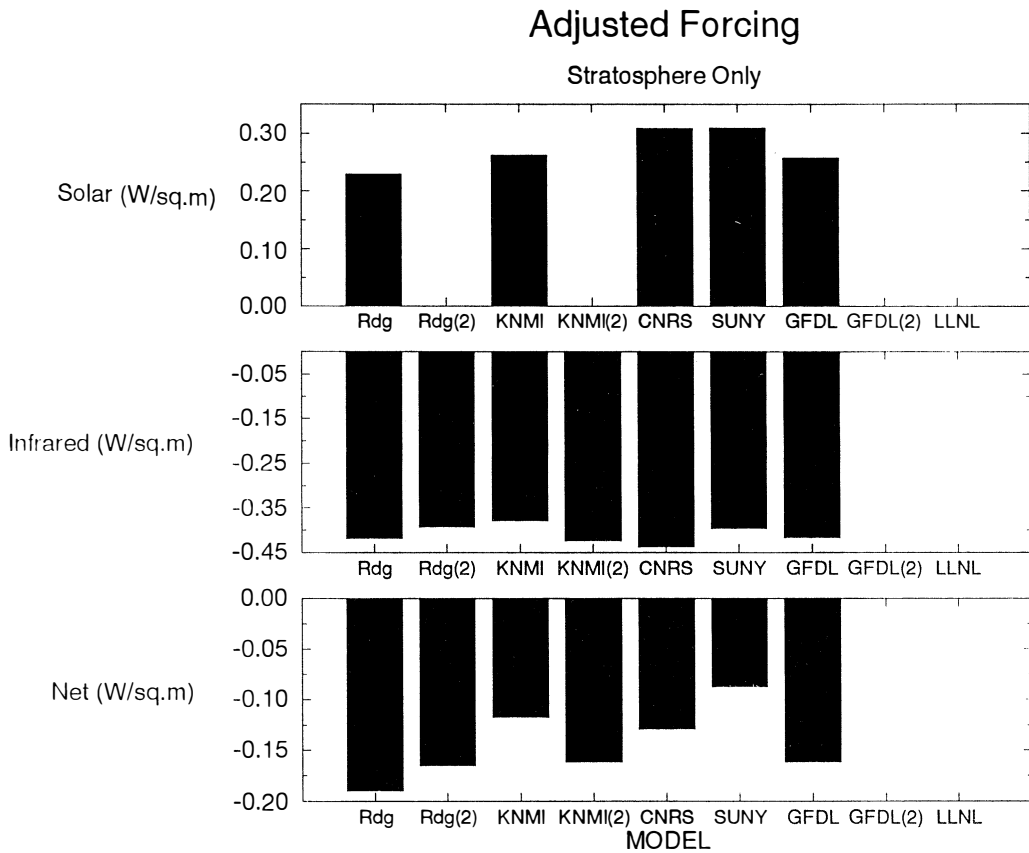


Figure 8-3. As in Figure 8-2, but after allowing for stratospheric temperature changes (“adjusted forcing” using Fixed Dynamical Heating) shown in Figure 8-4.

Figure 8-3 shows the changes in solar, thermal infrared, and net irradiances after allowing for stratospheric adjustment. The solar changes are only very slightly affected by the adjustment process, but the stratospheric cooling decreases the thermal infrared (and hence net) irradiance by typically 0.3 Wm^{-2} compared to the instantaneous case. The relative effect of the $14 \mu\text{m}$ band is less than in the instantaneous case, but it is more important in an absolute sense and contributes about -0.03 Wm^{-2} . All models now indicate that a decrease in lower stratospheric ozone leads to a cooling tendency for the surface-troposphere system, but the spread in the results is greater than for the instantaneous forcing (Figure 8-2).

Figure 8-4 shows the temperature changes calculated by each of the models; again there is a substantive spread. The effect of the adjustment process can be as-

certained by computing the change in the net irradiance between the instantaneous and adjusted calculations; the results agree to within 10%. This agreement is better than might be anticipated from Figure 8-4. However, calculations with the Reading model indicate that most of the change in net irradiance at the tropopause when adjustment was included came from the temperature changes within about 3 km of the tropopause; at these levels the temperature changes predicted by the models are in much better agreement.

The results were interpreted by Shine *et al.* (1994) as follows. About 50% of the modeled temperature change is due to the change in solar heating rates. Altitudes nearest the tropopause are most influenced by the longer wavelength (Chappuis) absorption bands of ozone; the models are in much better agreement about the change in these bands than the changes at shorter

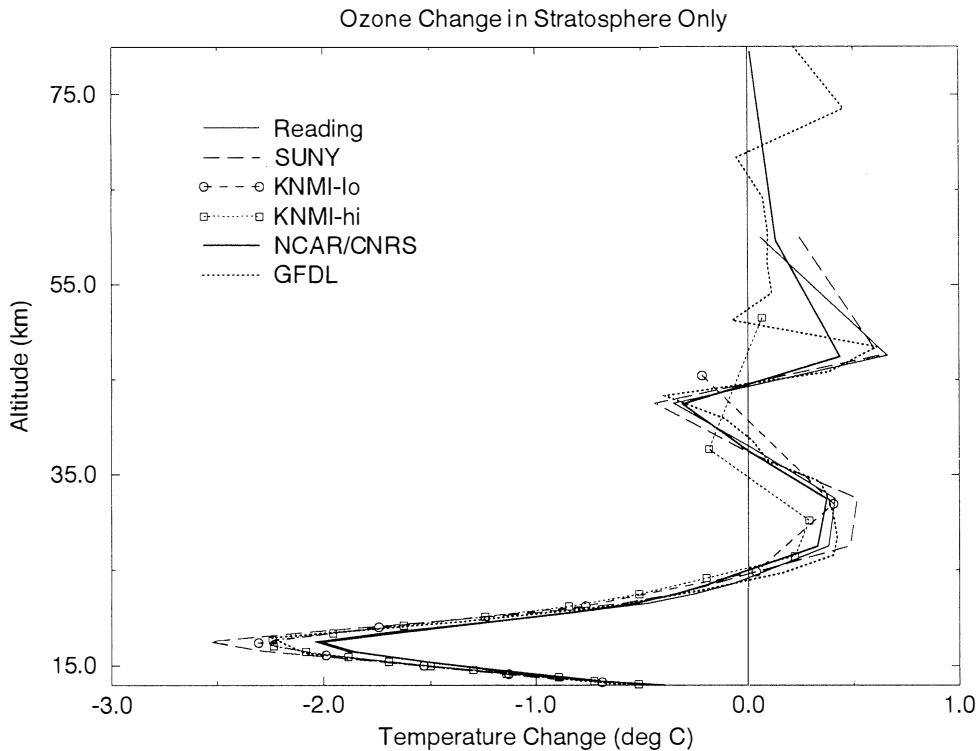


Figure 8-4. Change in stratospheric temperature (deg C) as a function of altitude computed by the participants in the Ozone Radiative Forcing Intercomparison for the change in stratospheric ozone shown in Figure 8-1. The Fixed Dynamical Heating approximation is used. The KNMI results are presented at two vertical resolutions.

wavelengths, so that the effect of adjustment is more similar in the models. The results can be brought into good agreement for the adjusted case by (i) adding the effect of the 14 μm band to those calculations that do not include it and (ii) using a single value of the solar irradiance change, rather than using the solar irradiance change calculated by each model independently. The major conclusion from this is that the main reason for inter-model differences is the way the solar forcing is calculated; it is this aspect of the calculations most in need of scrutiny in each model. As reported by Shine *et al.* (1994), high-resolution calculations of the solar irradiance change appear to be in good agreement; hence, the spread in shortwave results is not believed to represent the actual uncertainty in modeling irradiances, but is more a reflection of the simplifications used in existing parameterizations.

8.2.3 General Circulation Model Calculations

Hansen *et al.* (1992, 1994) have used a general circulation model (GCM) to evaluate the relative effects of changes in the well-mixed greenhouse gases and ozone upon the surface temperature. A sequence of model runs with the 1970-1990 increases in the well-mixed greenhouse gases only is compared with a sequence including observed stratospheric ozone changes; the members of each sequence differ only in their initial conditions. It is estimated that the 1970-1990 modeled surface warming (0.35 deg C) due to greenhouse gases is reduced by 15% due to the ozone changes (see Figure 8-5). There is a considerable spread among the different GCM realizations in the sequence of experiments performed; however, the results indicate that the cooling induced by ozone loss has the potential to reduce the warming effect due to the halocarbon increases over the time period considered. The results from this study are broadly

RADIATIVE FORCING

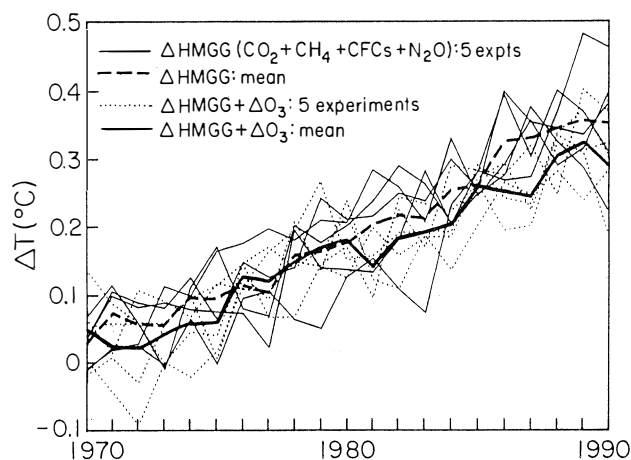


Figure 8-5. Transient global surface temperature change due to changes in greenhouse gases, as simulated by the GISS GCM (Hansen *et al.*, 1992, 1994). Five experiments were run with homogeneously mixed greenhouse gases (HMGG) (CO_2 , CH_4 , N_2O , and CFCs). Five additional experiments were run with an ozone change inferred from the Total Ozone Mapping Spectrometer (TOMS) and placed entirely in the 70-250 mb layer in addition to the changes in HMGG.

consistent with the expected temperature changes anticipated from the radiative forcing calculations.

Hansen *et al.* (1994) also investigate the climate sensitivity to changes in the vertical profile of ozone using a simplified 3-D model; all previous studies have used 1-D models. Such an investigation of parameter space would be difficult with a full GCM because of the computational cost. Instead, Hansen *et al.* use a sector version of the 9-level Goddard Institute for Space Studies (GISS) GCM they call the “Wonderland” Climate Model (see also Hansen *et al.*, 1993). The surface temperature response is a strong function of the height of the ozone change for two reasons. First, as is well-established (see Section 8.2.1), the radiative forcing is a strong function of the height of the ozone change; in addition, the climate sensitivity (*i.e.*, the surface warming per unit radiative forcing) is found to be a function of the height of the ozone change. This sensitivity is most marked in experiments that allow cloud feedbacks; in experiments with large and idealized perturbations in ozone, the climate sensitivity to changes in tropospheric ozone is substantially modified when cloud feedbacks are included.

The results of Hansen *et al.* (1994) have not yet been reported in detail and must be regarded as preliminary. In addition, the sensitivity to cloud feedbacks is likely to vary considerably amongst different GCMs because of the recognized difficulties in modeling clouds in GCMs (*e.g.*, IPCC, 1990, 1992). However, if confirmed by other studies, the new results could have very significant implications for the way the possible climatic impacts of ozone changes are assessed.

As discussed in IPCC (1994) available GCM simulations raise important, but as yet unresolved, issues about the way in which the global mean of a spatially very inhomogeneous radiative forcing, such as that due to ozone change, can be directly compared to the global-mean forcing due to, for example, changes in well-mixed greenhouse gases.

8.2.4 Attribution of Ozone Radiative Forcing to Particular Halocarbons

As discussed in earlier chapters, the weight of evidence suggests that heterogeneous chemical reactions involving halocarbons are the cause of the observed lower stratospheric ozone depletion. Since several of these compounds, particularly the CFCs, exert a (direct) positive radiative forcing, the (indirect) negative radiative forcing due to the chemically induced ozone loss has the potential to substantially reduce the overall contribution of the halocarbons to the global-mean greenhouse forcing, particularly over the past decade.

Daniel *et al.* (1994) have employed simplified chemical considerations and partitioned the total direct and the total indirect forcing among the various halocarbons (see also the discussion in Chapter 13 and Figure 13-9). The indirect effect is strongly dependent upon the effectiveness of each halocarbon for ozone destruction. On a per-molecule basis, bromine-containing compounds are estimated to contribute more to the indirect effect because they are more effective ozone depleters than chlorine-containing compounds, whilst the chlorinated compounds have a much bigger direct effect because they are stronger absorbers in the infrared. Thus for the total halocarbon forcing up to 1990, Daniel *et al.* estimate that the indirect effect of the CFCs is about 20% of the direct effect but has the opposite sign. For the halons, though, the (indirect) cooling effect is about 3 times larger than the warming due to the direct effect. Nevertheless, because of their greater concentrations,

the CFCs are estimated to have contributed about 50% of the total indirect forcing; the precise value depends on the value used for the effectiveness of bromine, relative to chlorine, at destroying ozone.

For the period 1980 to 1990, Daniel *et al.* attribute about 50% of the negative forcing to the CFCs, about 20% each to carbon tetrachloride and methyl chloroform, and about 10% to the bromocarbons. The net (direct plus indirect) forcing for the CFCs is about 50% of their direct effect, while the net forcing for carbon tetrachloride, methyl chloroform, and the bromocarbons is likely to have been negative.

The analysis suggests that the net forcing by halocarbons was probably quite strong in the 1960s and 1970s (see Figure 8-6); then, when the ozone decrease became more marked, the growth in the net forcing decreased substantially. Using projections for the change in halocarbons over the next century (based on the Copenhagen Amendment to the Montreal Protocol and projections of possible hydrofluorocarbon (HFC) use), Daniel *et al.* estimate that the cooling effect due to ozone depletion will soon begin to decrease; by the latter half of next century, the positive forcing due to HFCs will be the dominant contributor to the radiative forcing due to halocarbons.

8.2.5 Outstanding Issues

Radiative forcing due to a specified ozone change, as a function of the ozone altitude, is qualitatively well understood. However, as revealed by the intercomparison exercise, approximate radiative methods appear to differ in their estimates; it is important that such differences be understood. The principal limitation inhibiting an accurate estimate of the global ozone forcing is the lack of knowledge of the precise vertical profile of change with latitude and season.

In contrast to the well-mixed greenhouse gases, ozone change causes a more complicated radiative forcing – neither the ozone profile nor the change are uniform in the horizontal and vertical domains. The spatial patterns of the radiative forcing differ for changes in ozone and the well-mixed gases. Even the apportionment of the radiative forcing between the surface and the troposphere is different for ozone compared to the well-mixed greenhouse gases (WMO, 1986, 1992). Ozone forcings have not been used for systematic climate studies analogous to those carried out for the well-mixed

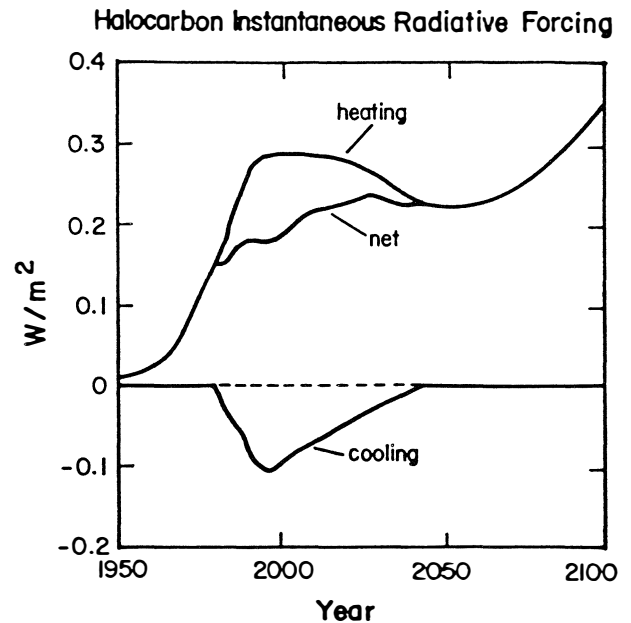


Figure 8-6. Radiative forcing (Wm^{-2}) due to changes in halocarbons (labeled “heating”) and an estimate of the associated stratospheric ozone loss (labeled “cooling”) and net change using observed halocarbon changes and an “optimistic” scenario based on the Copenhagen Amendment to the Montreal Protocol and assuming bromine is 40 times more effective at destroying ozone than chlorine. From Daniel *et al.* (1994).

greenhouse gases. A remaining question is the degree to which the irradiance change at the tropopause is a reasonable indicator of the surface temperature response in the case of ozone changes; it is for the well-mixed greenhouse gases, but preliminary work indicates that it may not be for ozone.

A further complication that needs to be explored is that changes in ozone in the vicinity of the tropopause have the potential to alter tropopause height. Thus, the energy received by the surface-troposphere system may be different in a model that allows changes in the tropopause height than in a model with a fixed tropopause. The vertical resolution of a model in the upper troposphere could then be an important consideration.

As discussed in earlier chapters, there is evidence that heterogeneous chemistry on sulfate aerosol leads to enhanced ozone loss. The observations of unusually low ozone in the northern midlatitudes during the winter of

RADIATIVE FORCING

1992-93 and spring of 1993 suggest a possible link with the Mt. Pinatubo aerosols. Such a volcano-ozone link would imply an enhancement of the transient negative radiative forcing owing to the presence of unusually large volcanic sulfate aerosol concentrations.

Additional complications in the determination of the ozone forcing are uncertainties in the feedbacks related to chemical processes. One example of this is the connection between stratospheric ozone loss, OH, and methane lifetimes. A depletion of stratospheric ozone would lead to an enhancement in tropospheric UV radiation, which in turn increases the rate of production of OH and destruction of methane (see, *e.g.*, Chapter 7 and Madronich and Granier [1992, 1994]). However, it is important to note that photochemical oxidation of methane and other species that react with OH takes place largely in the tropics, where ozone losses are small or not statistically significant. Thus a quantitative assessment of this effect requires consideration not only of tropospheric chemistry but also the latitudinal distribution of ozone depletion (particularly the tropical trends and the sensitivity to them). A cooling of the lower stratosphere due to the ozone loss can affect the water vapor mixing ratios there, with the potential to alter heterogeneous chemical reactions. Also, changes in methane in the stratosphere as a consequence of the altered tropospheric processes could be accompanied by changes in stratospheric water vapor that, in turn, would affect the radiation balance.

8.3 OBSERVED TEMPERATURE CHANGES

A large number of factors can influence stratospheric temperatures (see, *e.g.*, Randel and Cobb, 1994). Natural phenomena can result in a change in the radiative fluxes in the stratosphere, such as changes in solar output or in aerosols resulting from volcanic eruptions. Internal variability of the climate system, such as the quasi-biennial oscillation and the El Niño-Southern Oscillation, can induce dynamical effects that result in temperature change by advection and, if ozone changes as a result, also by radiative processes. Additionally, human activity is resulting in changes in a number of radiatively active constituents, such as ozone and carbon dioxide, and these can perturb the radiation balance and hence the temperature; attempts to detect trends due to human activity require consideration of the natural pro-

cesses. Most recent work on temperature trends has concentrated on the lower stratosphere, so we will concentrate on this region in this section; the particular emphasis will be on (i) the impact of Mt. Pinatubo and (ii) the detection of long-term trends.

8.3.1 Effects of the Volcanic Eruptions, Especially Mt. Pinatubo

A number of studies have reported the lower stratospheric warming following the eruption of Mt. Pinatubo (Labitzke and McCormick, 1992; Angell, 1993; Spencer and Christy, 1993; Christy and Drouilhet, 1994); this warming is associated with the increased absorption of upwelling thermal infrared radiation and solar radiation by the stratospheric aerosol layer (see, *e.g.*, WMO, 1988).

Angell (1993), from a selection of radiosonde stations, finds that the warming of the lower stratosphere following both Agung and El Chichón was greatest in the equatorial zone and least in the polar zones. The warming following El Chichón was slightly greater than following Agung everywhere except the south polar zone. Preliminary analysis for Mt. Pinatubo indicated that, in the north extratropics and the tropics, the warming following this eruption was comparable to the warming following Agung and El Chichón. However, in south temperate and south polar zones, the warming following Mt. Pinatubo is considerably greater, perhaps due to a contribution from the eruption of Volcán Hudson in Chile. Globally, the warming of the lower stratosphere following Mt. Pinatubo is greater than that following El Chichón and Agung.

Figure 8-7 (updated from Labitzke and Van Loon, 1994) shows the Northern Hemisphere annual area-weighted temperature series from an analysis of radiosonde data. The times of the Agung, El Chichón, and Mt. Pinatubo eruptions are marked, although it should be noted that other, less intense volcanic eruptions during this period probably led to some enhancement of the stratospheric aerosol load (*e.g.*, Robock, 1991; Sato *et al.*, 1993). Whilst the Northern Hemisphere post-Pinatubo warming is clear, particularly at 50 mbar, it is not obviously larger than that due to El Chichón.

More recently, satellite observations from Channel 4 of the Microwave Sounder Unit (MSU) on the NOAA polar-orbiting satellites have been used to monitor lower stratospheric temperatures (*e.g.*, Spencer and Christy,

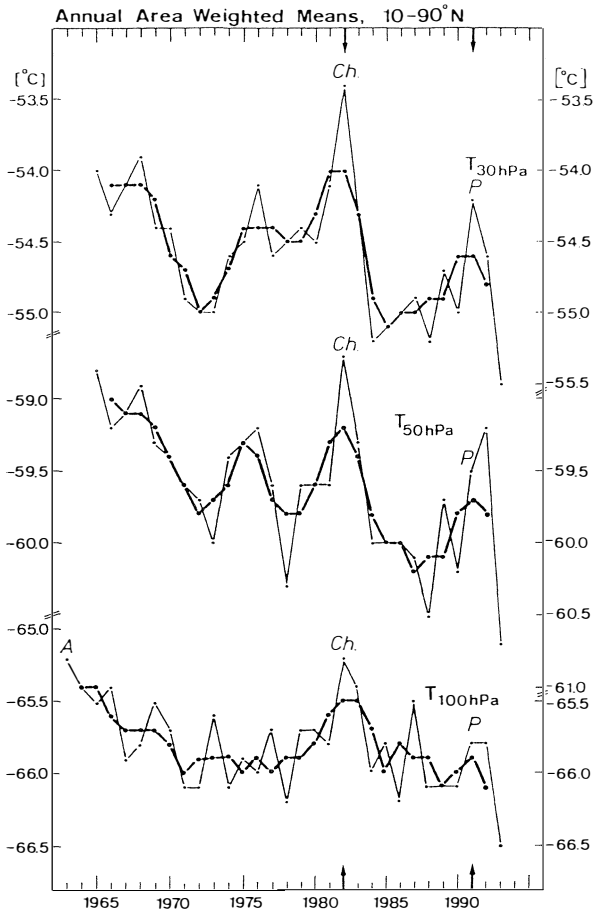


Figure 8-7. Annual mean area-weighted (10° - 90° N) temperatures ($^{\circ}$ C) at 30, 50, and 100 mb. The heavy lines are three-year running means. Based on daily radiosonde analysis by the Free University of Berlin (updated from Labitzke and Van Loon, 1994). A, Ch, and P denote the times of the Agung, El Chichón, and Mt. Pinatubo eruptions, respectively.

1993; Christy and Drouilhet, 1994; Randel and Cobb, 1994). The weighting function for Channel 4 peaks at about 75 mbar with half-power values at 120 and 40 mbar (Christy and Drouilhet, 1994). Figure 8-8 shows the global and hemispheric monthly-mean anomalies from MSU between January 1979 and July 1994 (J. Christy and R. Spencer, personal communication). From the global data set, Mt. Pinatubo gives a slightly greater warming (about 1.1 deg C in 1991/1992) than El Chichón (about 0.7 deg C in 1982/1983) compared to the immediate pre-eruption temperatures.

The Northern Hemisphere MSU Channel 4 data in Figure 8-8 can be compared with the radiosonde data analysis in Figure 8-7, although differences in the vertical resolution of the data sets need to be recognized. Both data sets are in general agreement that the immediate post-eruption warming is similar for both El Chichón and Mt. Pinatubo. The greater warming in the Southern Hemisphere following Mt. Pinatubo is consistent in both the MSU analysis (see Figure 8-8 and Christy and Drouilhet [1994]) and radiosonde analysis (Angell, 1993).

Hansen *et al.* (1993) show that the tropical warming in the lower stratosphere associated with Mt. Pinatubo is very well simulated by the GISS GCM with an imposed idealized volcanic aerosol cloud.

One interesting development in the identification of volcanic signals is the use of temperature and ozone data together (Randel and Cobb, 1994; A.J. Miller, personal communication). Normally, temperatures in the lower stratosphere and total ozone are positively correlated; Randel and Cobb show that this correlation changes sign when the lower stratospheric aerosol layer is enhanced as a result of volcanic eruptions.

8.3.2 Long-Term Trends

Both Figures 8-7 and 8-8 emphasize that the detection of long-term trends in temperatures in the lower stratosphere will be difficult because of the episodic and frequent volcanic eruptions that cause a major perturbation to those temperatures. An additional problem concerns the quality of available radiosonde data (see, *e.g.*, IPCC, 1992; Gaffen, 1994; Parker and Cox, 1994). Changes in instrumentation, ascent times, and reporting practices introduce a number of time-varying biases that have not yet been properly characterized; they indicate the need for some caution when using data primarily intended for weather forecasting for climate trend analysis. Nevertheless, since 1979, comparison of independent MSU Channel 4 data with radiosonde analyses in the lower stratosphere has shown good agreement (Oort and Liu, 1993; Christy and Drouilhet, 1994).

Considering all available radiosonde reports for the period December 1963 through November 1988, Oort and Liu (1993) infer a trend in the global lower stratospheric (100-50 mbar) temperature of -0.4 ± 0.12 deg C/decade; the cooling trend is apparent during all seasons and in both hemispheres. These results were

RADIATIVE FORCING

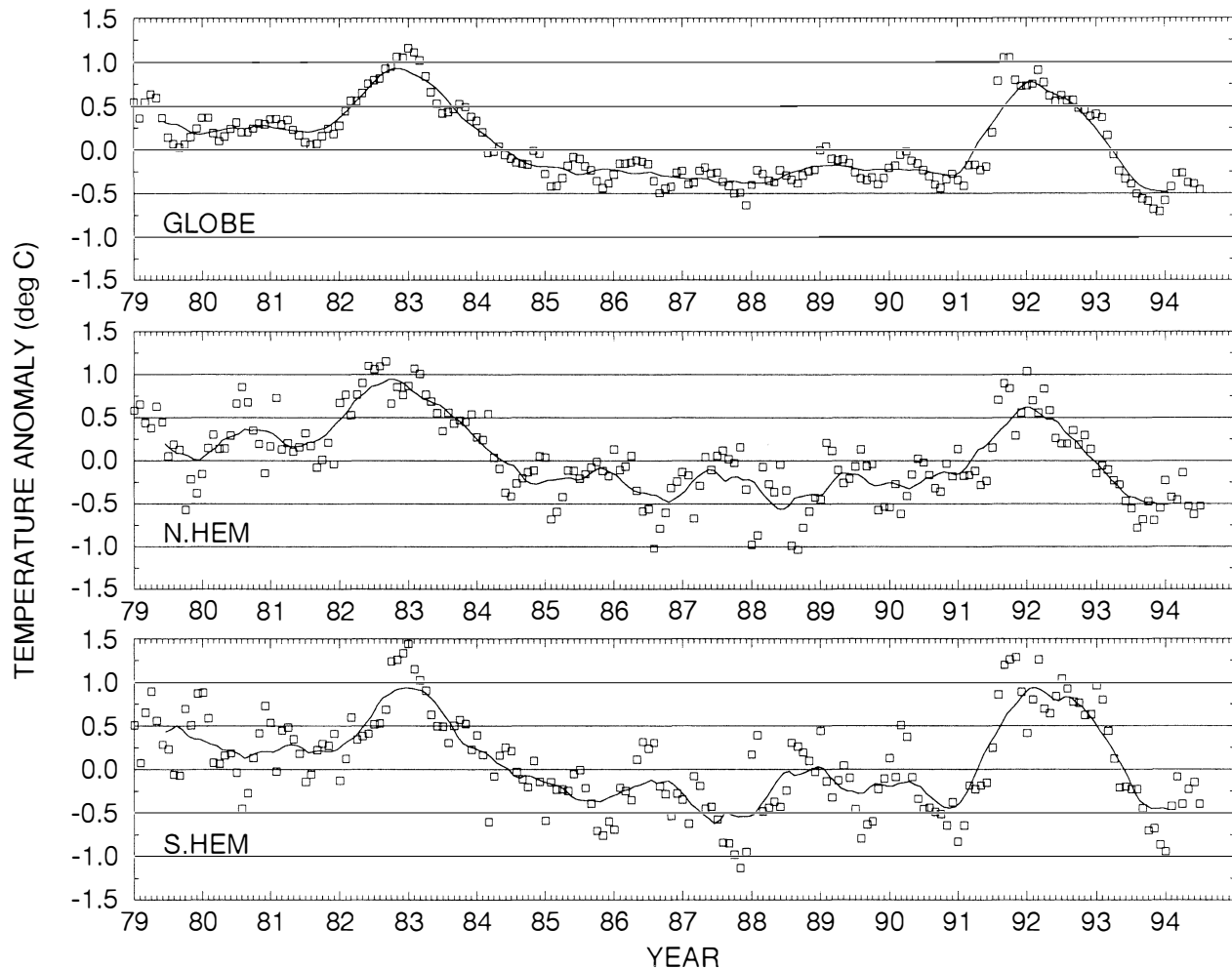


Figure 8-8. Global and hemispheric monthly-mean lower stratospheric temperature anomalies (from 1982-1991 means) from the MSU Channel 4 from January 1989 to July 1994. The solid line indicates the 12-month running mean. (Data from J.R. Christy and R. Spencer. See text for a description of the weighting function of MSU Channel 4.)

compared with earlier estimates by Angell (1988), who used a subset of 63 sonde stations, for the same time period; Oort and Liu find that their global and hemispheric trends agree with Angell's within the error bars, although Angell's larger Southern Hemisphere trends are believed to be associated with undersampling. These trend analyses are also consistent with the findings in Miller *et al.* (1992). IPCC (1992) combines the analysis of Oort and Liu with more recent data from Angell to deduce a global trend of -0.45 deg C/decade between 1964 and 1991 for the 100-50 mbar layer.

A concern expressed in IPCC (1992) was that trend analyses starting in 1964 may be biased by the warming associated with the eruption of Agung in 1963; however, Oort and Liu (1993) extend their own Northern Hemisphere analysis and Angell's global analysis back to December 1958 and find the decadal trends to differ little from those calculated for the period December 1963 to November 1988.

Latitudinal profiles of the estimated trends from Oort and Liu (1993) (see Figure 8-9) show that the cooling of the lower stratosphere has occurred everywhere,

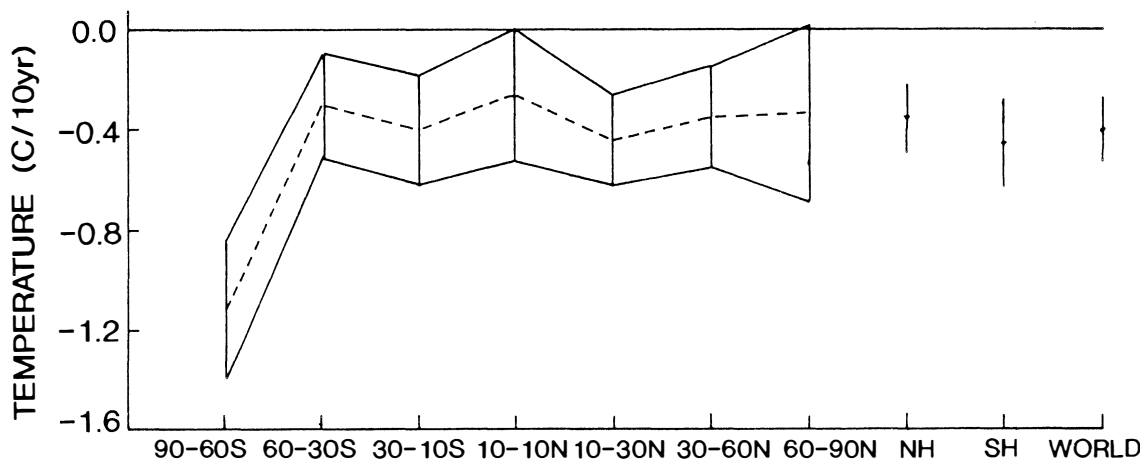


Figure 8-9. Latitudinal profiles of the estimated trends in the annual mean temperatures (in deg C/decade) from the GFDL radiosonde analysis (after Oort and Liu, 1993) for the 100-50 mb layer during the period December 1963 - November 1989. The 95% confidence limits are also shown. The hemispheric and global-mean changes are shown on the right of the figure.

but that the strongest temperature decreases (-1 deg C/decade) have occurred in the Southern Hemisphere extratropics, strongly suggesting an association with the Antarctic ozone hole.

Labitzke's (personal communication) analysis of Northern Hemisphere sonde data indicates an annual mean trend of -0.2 to -0.4 deg C/decade between 1965 and 1992 between 30 and 80 mbar at most latitudes; however, the trend varies greatly from month to month both in size and in sign, and is most difficult to detect in the extratropics during the Northern Hemisphere winter when interannual variability is substantial. This suggests that the winter months are best avoided for long-term trend detection. There is an indication that the trend during springtime is more negative over the period 1979-1993 than over the period 1965-1993. Figure 8-10 shows the analyses for May for these two periods; for substantial regions the trend is almost double for the later period, although it must be noted that the significance level is much lower, as it contains fewer data.

For the shorter period available from MSU Channel 4 observations, trends are clearly sensitive to the period of analysis (Figure 8-8); Christy and Drouilhet (1994) report a trend of -0.26 deg C/decade for the period January 1979 to November 1992, but comment that, because of the effects of the volcanoes, its significance is hard to assess. Downward trends are most marked for

the temperatures in the lower stratosphere of the polar cap regions (defined as being 67.5° to 83.5°), being -0.78 deg C/decade for the north polar cap and -0.90 deg C/decade for the south polar caps for the period January 1979 to January 1994 (J.R. Christy, personal communication).

For the period 1979-1991, Randel and Cobb (1994), using MSU data, infer a significant cooling of the lower stratosphere over the Northern Hemisphere midlatitudes in winter-spring (with a peak exceeding -1.5 deg C/decade) and over Antarctica in the Southern Hemisphere spring (peak exceeding -2.5 deg C/decade) (Figure 8-11); the overall space-time patterns are similar to those determined for ozone trends. The Northern Hemisphere trends derived from MSU data are in good agreement with the sonde analysis from the Free University of Berlin (McCormack and Hood, 1994; K. Labitzke, personal communication).

In summary, the available analyses continue to support the conclusions of WMO (1992) that the lower stratosphere has, on a global-mean basis, cooled by about 0.25 - 0.4 deg C/decade in recent decades, although more work on the quality of the archived data sets is clearly warranted.

In the upper stratosphere and mesosphere there is little new to report beyond the discussion in WMO (1992). Upper stratospheric temperature trends based on

RADIATIVE FORCING

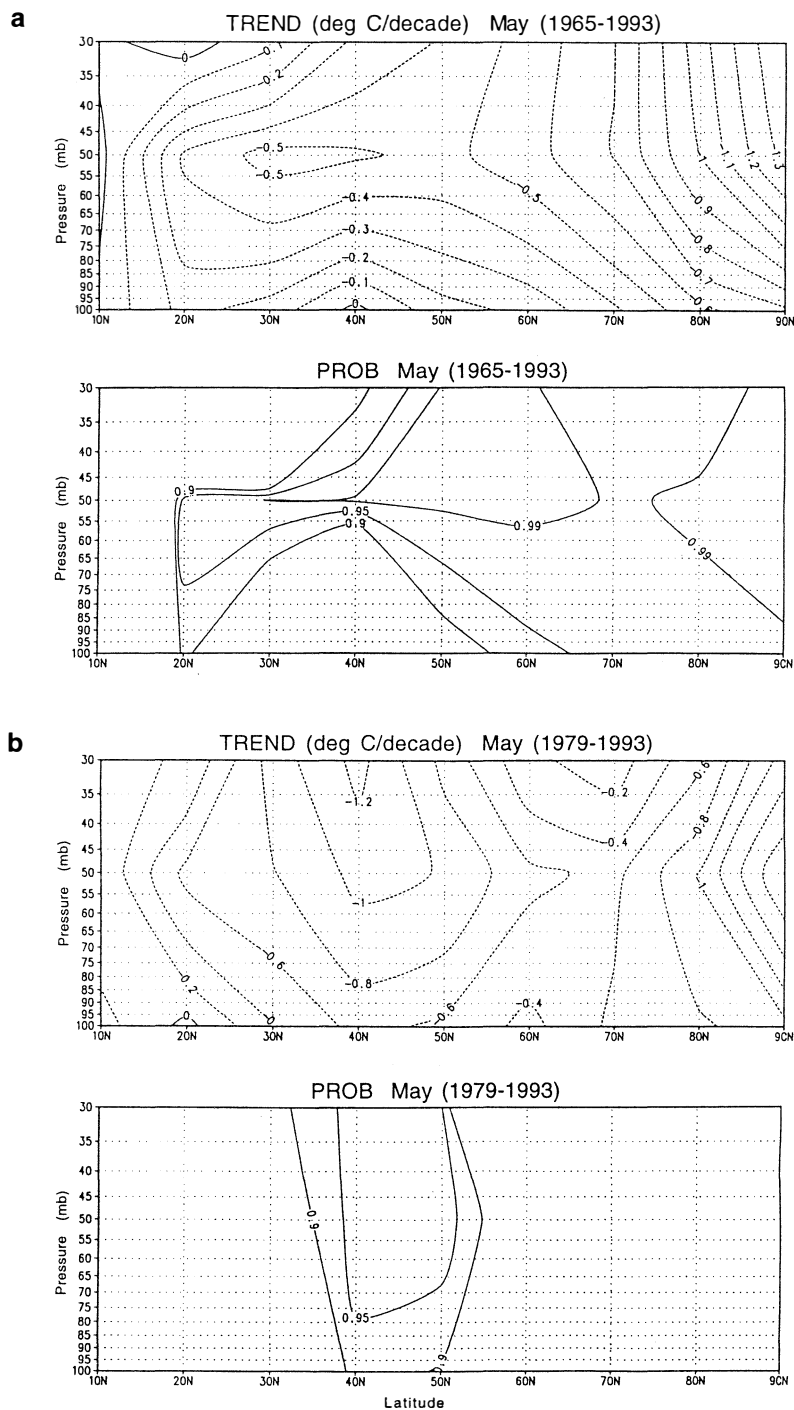


Figure 8-10. (a) Upper Panel—Northern Hemisphere temperature trend derived from radiosonde analyses (deg C/decade) in May for the period 1965-1993 based on data at 100, 50, and 30 mb levels. Lower Panel—lines of 90, 95, and 99% significance. (b) As (a) but for the period 1979-1993. (K. Labitzke, personal communication).

satellite, rocket, and lidar data do not lead to a clear conclusion concerning trends; mesospheric coolings of several deg C per decade in the past decade have been deduced (see also Chanin, 1993; Kokin and Lysenko, 1994).

8.3.3 Interpretation of Trends

Models indicate that the loss of ozone in the lower stratosphere leads to a decrease in the temperature there (WMO, 1992 and Section 8.2.1.1). One-dimensional models, such as the Fixed Dynamical Heating (FDH) and the Radiative-Convective Models, compute significant temperature changes of several tenths of a deg C/decade in the lower stratosphere due to the ozone changes of the past decade (WMO, 1992; Miller *et al.*, 1992; Shine, 1993; Karol and Frolkis, 1994; Ramaswamy and Bowen, 1994). It is this temperature change in the FDH models that determines, to a substantial extent, the negative forcing due to the ozone losses (see Section 8.2.1.1).

The cooling trends in the lower stratosphere, either from the long-term records or those over the past decade, are too negative to be attributable to increases in the well-mixed greenhouse gases (mainly CO₂) alone (Miller *et al.*, 1992; Hansen *et al.*, 1993; Shine, 1993; Ramaswamy and Bowen, 1994). In contrast, models employing the observed ozone losses yield a global temperature decrease that is broadly consistent with observations. This strongly suggests that, among the trace gases, stratospheric ozone change is the dominant contributor to the observed cooling trends. However, the potential competing effects due to unknown changes in other radiative constituents (*e.g.*, ice clouds, water vapor, tropospheric aerosols, and tropospheric ozone: Hansen *et al.*, 1993; Ramaswamy and Bowen, 1994) make it difficult to rigorously quantify the precise contribution by ozone to the temperature trends.

McCormack and Hood (1994) calculate the temperature decreases using an FDH model employing the ozone changes deduced from Solar Backscatter Ultraviolet (SBUV) observations for the period 1979-1991; the temperature changes are comparable to or slightly less than the decadal change inferred from satellite and radiosonde data in regions where the observed trends are statistically significant. Importantly, the modeled latitudinal and seasonal dependences are in reasonable agreement with the observations.

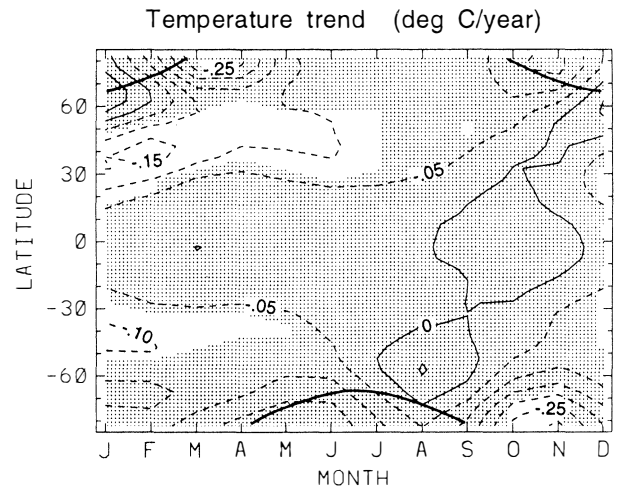


Figure 8-11. Latitude-time sections of zonal-mean lower stratospheric temperature trends in deg C/year calculated from MSU Channel 4 data (Randel and Cobb, 1994) for the period 1979-1991. Stippling denotes regions where the statistical fits are not different from zero at the 2σ level. (See text for description of the weighting function of MSU Channel 4.)

General circulation model (GCM) studies with imposed ozone losses in the lower stratosphere also obtain a temperature decrease in this region. Hansen *et al.* (1993) obtain a cooling in the lower stratosphere that is qualitatively consistent with and, in the global mean, agrees well with the decadal trend (-0.4 deg C) inferred from radiosonde observations. Another GCM study (V. Ramaswamy, personal communication) finds a similar cooling of the lower stratosphere and shows that the FDH temperature changes exhibit a qualitatively similar zonal pattern to the GCM results.

Mahlman *et al.* (1994) present a three-dimensional chemical-radiative-dynamical investigation of the climatic effects due to the Antarctic ozone losses. The transport of ozone and the ozone losses are handled explicitly, although the modeled Antarctic ozone loss is somewhat less than observed. There is a decrease of the lower stratospheric temperatures in the Southern Hemisphere that is consistent with the observed trends. An important aspect of the GCM calculations is that they simulate a slight cooling in the lower stratosphere at lower latitudes as a dynamical consequence of extratropical ozone depletion; this is in contrast to FDH models which

RADIATIVE FORCING

calculate temperature changes only at latitudes of ozone change. Thus the presence of equatorial cooling in observations (see, *e.g.*, Figure 8-9) cannot be used as a simple discriminator of whether ozone depletion has occurred in the equatorial lower stratosphere (see Chapter 1). In addition, the simulation of Mahlman *et al.* (1994) shows a dynamically induced heating in the Antarctic mid-stratosphere as a consequence of the loss of ozone in the lower stratosphere; such dynamical effects need to be taken into account when attempting to detect temperature trends from other causes, such as the increased concentrations of other greenhouse gases.

It is encouraging that both the FDH models and the GCMs yield a cooling in the lower stratosphere that is consistent with the magnitude inferred from observations. Precise agreement might not be expected as, in all the model studies, the temperature changes in the lower stratosphere are subject to uncertainties related to the assumed vertical and horizontal distribution of the ozone change and there are uncertainties in the observed trends.

8.4 HALOCARBON RADIATIVE FORCING

8.4.1 Comparison of IR Absorption Cross Sections

Since the review in the AFEAS (1989) report (see also Fisher *et al.*, 1990), further work on the absorption cross sections of halocarbons has been reported; this is particularly important for some of the HCFCs (hydrochlorofluorocarbons) and HFCs (hydrofluorocarbons), as some of the data used in earlier assessments were from a single source. Recent comparisons of strengths of many CFCs (chlorofluorocarbons) are presented in McDaniel *et al.* (1991), Cappellani and Restelli (1992), and Clerbaux *et al.* (1993) and are not repeated here. For newer HCFCs and HFCs, measurements are more limited and the available measurements are reviewed. Molecules that are created by the destruction of halocarbons have the potential to cause a radiative forcing, but their lifetimes are believed to be too short for them to be of importance (see Chapter 12); they are therefore not considered here.

Measurements of infrared (IR) cross sections are normally made using Fourier transform IR spectrometers

and, sometimes, grating spectrometers; spectral resolutions range from around 0.01 cm^{-1} to 0.1 cm^{-1} . Clerbaux *et al.* (1993) present a detailed error estimate with errors ranging from 1-2% for strong absorption and 3-4% for weak absorption. Cappellani and Restelli (1992) estimate an uncertainty of 2.5% and other workers estimate uncertainties of between 5 and 10%.

Table 8-2 lists the integrated absorption cross sections of measurements of HFCs and HCFCs known to the authors. Measurements for a number of these molecules, as well as a number of halogenated ethers used as anesthetics, are also reported by Brown *et al.* (1990); however, the absorption cross sections are reported for only a limited spectral region ($800 - 1200\text{ cm}^{-1}$) that neglects some important absorption features. Garland *et al.* (1993) report measurements in the region $770-1430\text{ cm}^{-1}$ of the absorption cross sections of HFC-236cb, HFC-236ea, and HFC-236fa, as well as the fluorinated ether E-134. Because the results are presented as relative cross sections, they are not included in Table 8-2; their integrated strengths are reported to be between 1.5 and 2.3 times stronger than CFC-11.

As examples of the degree of agreement in the near-room temperature measurements, for HCFC-123, HCFC-141b, and HCFC-142b the spread of results is more than 25% of the mean cross section; however, the spread between the results from the two published studies (Cappellani and Restelli, 1992; Clerbaux *et al.*, 1993) is generally smaller. For HFC-134a the spread is about 10%. Detailed descriptions, including temperatures and pressures of the measurements, are not available for all the data sets, so it is difficult to comment on the discrepancies. Except for HCFC-22, only Cappellani and Restelli (1992), Clerbaux *et al.* (1993), and Clerbaux and Colin (1994) have published the details of their measurements of HFC/HCFC cross sections and presented measurements for a range of temperatures. In general, the change in integrated cross section over the range of temperatures is less than 10%, although the two groups do not always agree on the sign of the temperature effect. The spread of results puts a limit on our knowledge of the accuracy with which the radiative forcing due to these gases can currently be modeled.

Table 8-2. Integrated absorption cross sections of HFC and HCFCs in units of $\times 10^{-17} \text{ cm}^{-1}(\text{molec cm}^{-2})^{-1}$.

Gas	Clerbaux ¹	Brühl ²	Gehring ³	Majid ³	Hurley ⁴	Cappellani ⁵	McDaniel ⁶
HCFC-22	10.0-10.3		8.9	9.5		10.9-10.3	8.3-9.0
HFC-23					12.7		
HFC-32					6.3		
HFC-41					1.7		
HCFC-123	12.2-12.9	13.6	9.5	10.6	12.5	13.1-12.8	
HCFC-124	14.4	14.8	15.1				
HFC-125	16.1	15.7	14.5				
HFC-134a	12.7-12.6	12.5	11.8	12.2	13.0	14.1-13.2	
HCFC-141b	6.8-7.8	9.0	6.5	7.1	7.6		
HCFC-142b	10.8-11.1	12.1	9.2	9.6	10.3	11.3-10.7	
HFC-143	7.0-6.9						
HFC-143a		11.4	12.7				
HFC-152a	7.1-6.9	5.9		6.1	7.3	7.5-6.9	
HCFC-225a	17.5-17.7						
HCFC-225b	16.5-15.6						
HFC-227ea		21.2					

1. Clerbaux *et al.* 1993; ranges correspond to values at 253 K and 287 K, respectively; where only one value is quoted, it is for 287 K. Measurements in spectral interval 600-1500 cm^{-1} at 0.03 cm^{-1} resolution. HFC-143 is from Clerbaux and Colin (1994).
2. C. Brühl, personal communication of room temperature measurements at Max-Planck Institute–Mainz; measurements over interval 500-1400 cm^{-1} approx. Values supplied in $\text{cm}^{-1}(\text{atm cm at 296 K})^{-1}$ – converted by multiplying by $296 \div (273 \times 2.687 \times 10^{19})$.
3. Reported in Fisher *et al.* (1990); measurements made at room temperature. Values reported as $\text{cm}^{-1}(\text{atm cm at STP})^{-1}$. Converted by multiplying by $1 \div 2.687 \times 10^{19}$. Some authors (Clerbaux *et al.*, 1993, and Cappellani and Restelli, 1992) convert assuming the gas amounts are atm cm at 296 K; we have been unable to resolve this with D. Fisher. If original units are indeed at 296 K instead of STP, the values in the above table should be multiplied by 1.08.
4. M. Hurley and T.J. Wallington, personal communication of measurements by Ford; integrated cross sections derived by S. Pinnock (University of Reading). Measurements in spectral interval 700-3800 cm^{-1} at 0.12 cm^{-1} resolution at 296 K; estimated uncertainty is 5%. Experimental set-up described in Wallington *et al.* (1989).
5. Cappellani and Restelli, 1992. Range corresponds to values at 233K and 293 K. Measurements in spectral interval 600-1500 cm^{-1} at 0.01 cm^{-1} .
6. McDaniel *et al.*, 1991. Range corresponds to values at 203 K and 296 K. Measurements in spectral interval 600 - 1500 cm^{-1} at 0.03 cm^{-1} .

RADIATIVE FORCING

8.4.2 Comparison of Radiative Forcing Calculations

In IPCC (1990, 1992, 1994) a specific definition of radiative forcing was adopted such that:

The radiative forcing of the surface-troposphere system (due to a change, for example, in greenhouse gas concentration) is the change in net irradiance (in Wm^{-2}) at the tropopause after allowing for stratospheric temperatures to re-adjust to radiative equilibrium.

The tropopause is chosen because, in simple models at least, it is considered that in a global and annual-mean sense, the surface and troposphere are so closely coupled that they behave as a single thermodynamic system (see, *e.g.*, Rind and Lacis, 1993; IPCC, 1994) This follows earlier work (*e.g.*, Ramanathan *et al.*, 1985, Hansen *et al.*, 1981, and references therein). One advantage of allowing for the stratospheric adjustment is that the change in the net irradiance at the top of the atmosphere is then the same as the change at the tropopause; this is not the case when stratospheric temperatures are not adjusted (see Hansen *et al.*, 1981).

In preparing this review some difficulty has been experienced in intercomparing work performed by different authors, because some have applied the term “radiative forcing” to the instantaneous change in tropopause irradiance, not allowing for any change in stratospheric temperature. In other works, it is not clear which definition of radiative forcing has been adopted. It is also emphasized here that the forcing should be calculated as a global mean using appropriate vertical profiles of temperature, trace gas concentrations, and cloud conditions – again, it is not always clear, in published estimates, what conditions are being used for calculations. An added problem is that if perturbations used to calculate the forcings are too small, the results can be affected by computer precision, an effect that will vary between models, depending on their construction. Finally, when results are presented as ratios of forcings to other gases (*e.g.*, CO_2 or CFC-11) rather than as absolute forcings (*e.g.*, as $\text{Wm}^{-2} \text{ppbv}^{-1}$), it is important to know the absolute forcing of the reference gas to rigorously intercompare different works. Again, such information is not always presented.

The first calculations of the radiative forcing due to a large range of HFCs and HCFCs were reported in

Fisher *et al.* (1990). More recent calculations include those of Shi (1992), Brühl (personal communication), Clerbaux *et al.* (1993) and Clerbaux and Colin (1994); C. Granier (personal communication) has updated the Clerbaux *et al.* (1993) calculations to account for the effect of clouds, and these new values are used here. The results from these sources differ in general, because of the use of different radiation schemes, different spectroscopic data, different assumptions about vertical profiles of temperatures, clouds, etc., and whether stratospheric adjustment was included.

The Fisher *et al.* (1990) values for this class of gases were instantaneous forcings. The effect of adjustment can be estimated from the 1-dimensional radiative-convective model values in Fisher *et al.* (1990) (see footnote to Table 8-3). The adjustment leads to the adjusted forcing being up to 10% greater than the instantaneous forcing because an increase in the concentrations of these gases generally leads to a warming of the lower stratosphere, increasing the downwelling thermal infrared irradiance at the tropopause. The values most affected are those for the more heavily fluorinated gases (such as HFC-125 and HFC-134a).

Table 8-3 lists recent estimates of the strengths of the HFC and HCFCs, on a per-molecule basis, relative to CFC-11. The variations of the relative forcings from different studies show little consistency. The same spectral data in different radiation schemes do not always give the same relative forcings amongst the HFCs and HCFCs; and schemes using different spectral data do not always show differences that would be anticipated from the cross sections used. For the majority of gases, Shi (1992) computes a radiative forcing weaker than those given in IPCC (1990), by as much as 30% for HFC-125. The results from Brühl and Clerbaux *et al.* generally show no systematic difference compared with the Atmospheric and Environmental Research, Inc. (AER) values. For only two gases is there a consistent and large deviation from AER values: HFC-125 and HFC-152a.

More systematic work needs to be done to establish the effect of factors such as overlap with other species, stratospheric adjustment, the vertical profile of the absorber, and the dependence of the calculation on the spectral resolution, if the range in the current estimates is to be understood better.

Table 8-4 presents our recommended forcings for a wide range of gases, all relative to CFC-11. We have

Table 8-3. Radiative forcing due to HFC and HCFCs on a per-molecule basis relative to CFC-11 for gases for which more than one assessment is available.

Gas	AER ¹	AER adj ²	Du Pont ³	Shi ⁴	Brühl ⁵	Granier ⁶
HCFC-22	0.86	0.92	0.80	0.75	0.79	0.87
HCFC-123	0.80	0.82	0.69	0.67	0.80	0.89
HCFC-124	0.87	0.93	0.81	0.88	0.95	0.93
HFC-125	1.08	1.19	0.89/0.93	0.74	0.91	0.90
HFC-134a	0.77	0.84	0.71	0.65	0.66	0.78
HCFC-141b	0.62	0.64	0.57	0.64	0.68	0.65
HCFC-142b	0.82	0.89	0.76	0.63	0.93	0.81
HFC-143a	0.63	0.68	0.65	0.50	0.58	
HFC-152a	0.53	0.56	0.44/0.46	0.44	0.48	0.49
HFC-227ea			-1.24		1.09	

1. AER results from Fisher *et al.* (1990). They are instantaneous forcings.
2. AER-adjusted forcings deduced from results in Fisher *et al.* (1990), Tables 3 and 4. These authors wrote the climate sensitivity λ in terms of instantaneous forcing so that the surface temperature change equals λ times the instantaneous forcing. The climate sensitivity is reasonably independent of gas when using the adjusted forcing (*e.g.*, Rind and Lacis, 1993). The adjusted forcing, relative to CFC-11, can be estimated by multiplying the instantaneous forcing relative to CFC-11 by the ratio of the instantaneous sensitivity of a given gas to the instantaneous sensitivity for CFC-11.
3. Du Pont forcings from Fisher *et al.* (1990). They are instantaneous forcings. The adjusted forcings could be deduced as for the AER forcings above. Second values, where quoted, are more recent values from D. Fisher (personal communication).
4. From Shi (1992) and includes overlap with methane and nitrous oxide using spectral data from Fisher *et al.* (1990). The calculations are not believed to include stratospheric adjustment.
5. From C. Brühl (personal communication) using MPI-Mainz absorption cross sections and including overlap with methane and nitrous oxide.
6. From C. Granier (personal communication) using measurements from Clerbaux *et al.* (1993). The results include clouds and do not include stratospheric adjustment; the original Clerbaux *et al.* values were for clear skies.

chosen to retain values used in IPCC (1990) where there was neither a large nor a consistent deviation from more recent calculations. We replace the earlier values for HFC-125 and HFC-152a by those from C. Granier (personal communication). In cases where details of calculations have not been provided, we simply take the means of available estimates. It is subjectively estimated that these values are accurate to within about 25%, but it is anticipated that further revision will be necessary in the future. Another feature of Table 8-4 is that an attempt is made to classify HFC/HCFC species on the basis of likely emissions (using information from A. McCulloch [personal communication]).

Estimates for the forcing due to increased concentrations of HFCs and HCFCs between 1990 and 2100 include 0.15 Wm^{-2} by Daniel *et al.* (1994) and between 0.2 and 0.4 Wm^{-2} by Wigley (1994). For the sets of assumptions used by these authors, the forcing is a small fraction of the estimates of forcing due to increases in the well-mixed greenhouse gases between 1990 and 2100; the various scenarios used in IPCC (1992) give that forcing to lie between 3.4 and 8.5 Wm^{-2} . The actual radiative forcing due to future emissions of the HFCs and HCFCs depends critically on factors such as growth rates in emissions and the precise mix of species used.

RADIATIVE FORCING

Table 8-4. Radiative forcing relative to CFC-11 per unit mass and per molecule change in the atmosphere. The table shows direct forcings only. The absolute radiative forcing due to CFC-11 is taken from IPCC 1990 and is 0.22 dX Wm⁻², where dX is the perturbation to the volume mixing ratio of CFC-11 in ppbv.

GAS	Forcing per		Source	
	unit mass	molecule		
CFCs and other controlled chlorinated species				
CFC-11	CFCl ₃	1.00	1.00	IPCC (1990)
CFC-12	CF ₂ Cl ₂	1.45	1.27	IPCC (1990)
CFC-113	CF ₂ ClCFCl ₂	0.93	1.27	IPCC (1990)
CFC-114	CF ₂ ClCF ₂ Cl	1.18	1.47	IPCC (1990)
CFC-115	CF ₃ CF ₂ Cl	1.04	1.17	IPCC (1990)
*Carbon tetrachloride	CCl ₄	0.41	0.46	IPCC (1990)
Methyl chloroform	CH ₃ CCl ₃	0.23	0.22	IPCC (1990)
HFC/HFCs in production now and likely to be widely used				
HCFC-22	CHF ₂ Cl	1.37	0.86	IPCC (1990)
HCFC-141b	CH ₃ CFCl ₂	0.73	0.62	IPCC (1990)
HCFC-142b	CH ₃ CF ₂ Cl	1.12	0.82	IPCC (1990)
HFC-134a	CF ₃ CH ₂ F	1.04	0.77	IPCC (1990)
*HFC-32	CH ₂ F ₂	1.06	0.40	Fisher (personal communication)
HFC/HFCs in production now for specialized end use				
HCFC-123	CF ₃ CHCl ₂	0.72	0.80	IPCC (1990)
HCFC-124	CF ₃ CHFCI	0.88	0.87	IPCC (1990)
*HFC-125	CF ₃ CHF ₂	1.03	0.90	Granier (personal communication)
HFC-143a	CH ₃ CF ₃	1.03	0.63	IPCC (1990)
*HFC-152a	CH ₃ CHF ₂	1.02	0.49	Granier (personal communication)
*HCFC-225ca	CF ₃ CF ₂ CHCl ₂	0.72	1.07	Granier (personal communication)
*HCFC-225cb	CClF ₂ CF ₂ CHClF	0.87	1.29	Granier (personal communication)
HFC/HFCs under consideration for specialized end use				
*HFC-23 (+)	CHF ₃	1.59	0.81	Fisher (personal communication)
*HFC-134	CHF ₂ CHF ₂	1.08	0.80	Fisher (personal communication)
*HFC-143	CH ₂ FCHF ₂	0.85	0.52	Clerbaux and Colin (1994)
*HFC-227	CF ₃ CHFCF ₃	0.95	1.17	Mean of Brühl and Fisher (pers. comms.)
*HFC-236	CF ₃ CH ₂ CF ₃	1.06	1.17	Fisher (personal communication)
*HFC-245	CHF ₂ CF ₂ CFH ₂	0.95	0.93	Fisher (personal communication)
*HFC-43-10mee	C ₅ H ₂ F ₁₀	0.86	1.58	Fisher (personal communication)
Fully fluorinated substances				
*CF ₄		0.69	0.44	Isaksen <i>et al.</i> (1992)
*C ₂ F ₆		1.36	1.37	Isaksen <i>et al.</i> (1992)
*C ₃ F ₈		0.77	1.05	Brühl (personal communication)
*perfluorocyclobutane	cC ₄ F ₈	1.00	1.46	Fisher (personal communication)
*C ₆ F ₁₄		0.75	1.84	Mean of Brühl and Ko (pers. comms.)
*SF ₆		2.75	2.92	Mean of Ko <i>et al.</i> (1993)/Stordal <i>et al.</i> (1993)
Other species				
CFC-13	CClF ₃	1.37	1.04	Mean of Brühl and Fisher (pers. comms.)
CHCl ₃		0.09	0.078	Fisher (personal communication)
CH ₂ Cl ₂		0.23	0.14	Fisher (personal communication)
halon 1301	CF ₃ Br	1.19	1.29	IPCC (1990)
*CF ₃ I		1.20	1.71	Pinnock (personal communication)

+ Also emitted as a by-product of other halocarbon production

* Indicates value amended from IPCC 1990, or gas not previously listed; the mass factor for CCl₄ has altered due to a typographical error in IPCC 1990.

REFERENCES

- AFEAS, Alternative Fluorocarbons Environmental Acceptability Study, *AFEAS Report – Appendix (Volume 2) of Scientific Assessment of Stratospheric Ozone: 1989*, World Meteorological Organization Global Ozone Research and Monitoring Project – Report No. 20, Geneva, 1989.
- Angell, J.K., Variations and trends in tropospheric and stratospheric global temperatures, 1958-1987, *J. Climate*, *1*, 1296-1313, 1988.
- Angell, J.K., Comparison of stratospheric warming following Agung, El Chichón and Pinatubo volcanic eruptions, *Geophys. Res. Lett.*, *20*, 715-718, 1993.
- Briegleb, B.P., Longwave band model for thermal radiation in climate studies, *J. Geophys. Res.*, *97*, 11475-11485, 1992.
- Brown, A.C., C.-E. Canosa-Mas, A.D. Parr, and R.P. Wayne, Laboratory studies of some halogenated ethanes and ethers: Measurements of rates of reaction with OH and of infrared absorption cross sections, *Atmos. Environ.*, *24A*, 2499-2511, 1990.
- Cappellani, F., and G. Restelli, Infrared band strengths and their temperature dependence of the hydrohalocarbons HFC-134a, HFC-152a, HCFC-22, HCFC-123 and HCFC-142b, *Spectrochimica Acta*, *48A*, 1127-1131, 1992.
- Chanin, M.-L., Long-term trend in the middle atmosphere temperature, in *The Role of the Stratosphere in Global Change*, edited by M.-L. Chanin, NATO-ASI Series, Springer-Verlag, Berlin, 301-317, 1993.
- Christy, J.R., and S.J. Drouilhet, Variability in daily, zonal mean lower stratospheric temperatures, *J. Climate*, *7*, 106-120, 1994.
- Clerbaux, C., R. Colin, P.C. Simon, and C. Granier, Infrared cross sections and global warming potentials of 10 alternative hydrohalocarbons, *J. Geophys. Res.*, *98*, 10491-10497, 1993.
- Clerbaux, C., and R. Colin, Determination of the infrared cross section and global warming potential of 1,1,1-trifluoroethane (HFC-143), *Geophys. Res. Lett.*, *21*, 2377-2380, 1994.
- Daniel, J.S., S. Solomon, and D.L. Albritton, On the evaluation of halocarbon radiative forcing and global warming potentials, *J. Geophys. Res.*, in press, 1994.
- Fisher, D.A., C.H. Hales, W.-C. Wang, M.K.W. Ko, and N.-D. Sze, Model calculations of the relative effects of CFCs and their replacements on global warming, *Nature*, *344*, 513-516, 1990.
- Fishman, J., The global consequences of increasing tropospheric ozone concentrations, *Chemosphere*, *22*, 685-695, 1991.
- Gaffen, D.J., Temporal inhomogeneities in radiosonde temperature records, *J. Geophys. Res.*, *99*, 3667-3776, 1994.
- Garland, N.L., L.J. Medhurst, and H.H. Nelson, Potential chlorofluorocarbon replacements: OH reaction rate constants between 250 and 315 K and infrared absorption spectra, *J. Geophys. Res.*, *98*, 23107-23111, 1993.
- Grossman, A.S., K.E. Grant, and D.J. Wuebbles, Radiative flux calculations at UV and visible wavelengths, LLNL Report UCRL-ID-115336, Lawrence Livermore National Laboratory, Livermore, California, 1993.
- Grossman, A.S., and K.E. Grant, A correlated k-distribution model of the heating rates for atmospheric mixtures of H₂O, CO₂, O₃, CH₄ and N₂O in the 0-2500 cm⁻¹ wavenumber region at altitudes between 0-60 km, in *Proceedings of the 8th Conference on Atmospheric Radiation*, American Meteorological Society, Boston, Massachusetts, 97-99, 1994.
- Hansen, J., D. Johnson, A. Lacis, S. Lebedeff, P. Lee, D. Rind, and G. Russel, Climate impacts of increasing carbon dioxide, *Science*, *213*, 957-966, 1981.
- Hansen, J., W. Rossow, and I. Fung, Long-term monitoring of global climate forcing and feedbacks, *NASA Conference Publications 3234*, National Aeronautics and Space Administration, Washington, D.C., 1992.
- Hansen, J., A. Lacis, R. Ruedy, M. Sato, and H. Wilson, How sensitive is the world's climate?, *National Geographic Research and Exploration*, *9*, 142-158, 1993.

RADIATIVE FORCING

- Hansen, J., M. Sato, A. Lacis, and R. Ruedy, The impact on climate of ozone change and aerosols, in *Proceedings of IPCC Hamburg Meeting*, a joint workshop of IPCC Working Group I and the International Ozone Assessment Panel, Hamburg, available from IPCC WGI Technical Support Unit, Hadley Center, Meteorological Office, Bracknell, UK, 1994.
- Hauglustaine, D.A., C. Granier, G.P. Brasseur, and G. Mégie, The importance of atmospheric chemistry in the calculation of radiative forcing on the climate system, *J. Geophys. Res.*, *99*, 1173-1186, 1994.
- IPCC, *Climate Change. The IPCC Scientific Assessment*, Intergovernmental Panel on Climate Change, Cambridge University Press, 1990.
- IPCC, *Climate Change 1992. The Supplementary Report to the IPCC Scientific Assessment*, Intergovernmental Panel on Climate Change, Cambridge University Press, 1992.
- IPCC, *Radiative Forcing of Climate Change. An Interim Scientific Assessment*, Intergovernmental Panel on Climate Change, to be published by Cambridge University Press, 1994.
- Isaksen, I.S.A., C. Brühl, M. Molina, H. Schiff, K. Shine, and F. Stordal, An assessment of the role of CF₄ and C₂F₆ as greenhouse gases, Center for International Climate and Research, University of Oslo Policy Note 1992:6, 1992.
- Karol, I., and V.A. Frolkis, Model evaluation of the radiative and temperature effects of the ozone content changes in the global atmosphere of the 1980s, in *Proceedings of the Quadrennial Ozone Symposium 1992*, Charlottesville, Virginia, 13 June 1992, NASA Conference Publication CP-3266, 409-412, 1994.
- Kiehl, J.T., R.J. Wolski, B.P. Briegleb, and V. Ramanathan, Documentation of radiation and cloud routines in the NCAR Community Climate Model, NCAR Technical Note TN-288+IA, National Center for Atmospheric Research, Boulder, Colorado, 1987.
- Ko, M.K.W., N.-D. Sze, W.-C. Wang, G. Shia, A. Goldman, F.J. Murcray, D.G. Murcray, and C.P. Rinsland, Atmospheric sulfur hexafluoride: Sources, sinks and greenhouse warming, *J. Geophys. Res.*, *98*, 10499-10507, 1993.
- Kokin, G.A., and E.V. Lysenko, On temperature trends of the atmosphere from rocket and radiosonde data, *J. Atmos. Terr. Phys.*, *56*, 1035-1044, 1994.
- Labitzke, K., and M.P. McCormick, Stratospheric temperature increases due to Pinatubo aerosols, *Geophys. Res. Lett.*, *19*, 207-210, 1992.
- Labitzke, K., and H. Van Loon, A note on trends in the stratosphere: 1958-1992, *COSPAR Colloquia Series*, *5*, Pergamon Press, 537-546, 1994.
- Lacis, A.A., and J.E. Hansen, A parameterization for the absorption of solar radiation in the earth's atmosphere, *J. Atmos. Sci.*, *31*, 118-133, 1974.
- Lacis, A.A., D.J. Wuebbles, and J.A. Logan, Radiative forcing of climate by changes in the vertical distribution of ozone, *J. Geophys. Res.*, *95*, 9971-9981, 1990.
- McCormack, J.P., and L.L. Hood, Relationship between ozone and temperature trends in the lower stratosphere: Latitudinal and seasonal dependences, *Geophys. Res. Lett.*, *21*, 1615-1618, 1994.
- McDaniel, A.H., C.A. Cantrell, J.A. Davidson, R.E. Shetter, and J.G. Calvert, The temperature dependent infrared absorption cross sections for chlorofluorocarbons: CFC-11, CFC-12, CFC-13, CFC-14, CFC-22, CFC-113, CFC-114 and CFC-115, *J. Atmos. Chem.*, *12*, 211-227, 1991.
- Madronich, S., and C. Granier, Impact of recent total ozone changes on tropospheric ozone photodissociation, hydroxyl radicals and methane trends, *Geophys. Res. Lett.*, *19*, 465-467, 1992.
- Madronich, S., and C. Granier, Tropospheric chemistry changes due to increased UV-B radiation, in *Stratospheric Ozone Depletion—UV-B Radiation in the Biosphere*, edited by R.H. Biggs and M.E.B. Joyner, Springer-Verlag, Berlin, 3-10, 1994.
- Mahlman, J.D., J.P. Pinto, and L.J. Umscheid, Transport, radiative and dynamical effects of the Antarctic ozone hole: A GFDL "SKYHI" model experiment, *J. Atmos. Sci.*, *51*, 489-509, 1994.
- Marengo, A., H. Gouget, P. Nédelec, J-P. Pagés, and F. Karcher, Evidence of a long-term increase in tropospheric ozone from Pic du Midi data series – consequences: Positive radiative forcing, *J. Geophys. Res.*, *99*, 16617-16632, 1994.

- Miller, A.J., R.M. Nagatani, G.C. Tiao, X.F. Niu, G.C. Reinsel, D. Wuebbles, and K. Grant, Comparisons of observed ozone and temperature trends in the lower stratosphere, *Geophys. Res. Lett.*, *19*, 929-932, 1992.
- Morcrette, J.J., Radiation and cloud radiative properties in the ECMWF forecasting system, *J. Geophys. Res.*, *96*, 9121-9132, 1991.
- Oort, A.H., and H. Liu, Upper air temperature trends over the globe, 1958-1989, *J. Climate*, *6*, 292-307, 1993.
- Parker, D.E., and D.I. Cox, Towards a consistent global climatological rawinsonde data base, *Int. J. Climatology*, in press, 1994.
- Ramanathan, V., R.J. Cicerone, H.B. Singh, and J.T. Kiehl, Trace gas trends and their potential role in climate change, *J. Geophys. Res.*, *90*, 5547-5566, 1985.
- Ramaswamy, V., M.D. Schwarzkopf, and K.P. Shine, Radiative forcing of climate from halocarbon-induced global stratospheric ozone loss, *Nature*, *355*, 810-812, 1992.
- Ramaswamy, V., and M.M. Bowen, Effect of changes in radiatively active species upon the lower stratospheric temperatures, *J. Geophys. Res.*, 18909-18921, 1994.
- Randel, W.J., and J.B. Cobb, Coherent variations of monthly mean total ozone and lower stratospheric temperature, *J. Geophys. Res.*, *99*, 5433-5447, 1994.
- Rind, D., and A. Lacis, The role of the stratosphere in climate change, *Surveys in Geophysics*, *14*, 133-165, 1993.
- Robock, A., The volcanic contribution to climate change of the past 100 years, in *Greenhouse Gas Induced Climatic Change: A Critical Appraisal of Simulations and Observations*, edited by M.E. Schlesinger, Elsevier, Amsterdam, 429-443, 1991.
- Sato, M., J.E. Hansen, M.P. McCormick, and J.B. Pollack, Stratospheric aerosol optical depths, 1850-1990, *J. Geophys. Res.*, *98*, 22987-22994, 1993.
- Schwarzkopf, M.D., and S.B. Fels, The simplified exchange method revisited: An accurate, rapid method for computation of infrared cooling rates and fluxes, *J. Geophys. Res.*, *96*, 9075-9096, 1991.
- Schwarzkopf, M.D., and V. Ramaswamy, Radiative forcing due to ozone in the 1980s: Dependence on altitude of ozone change, *Geophys. Res. Lett.*, *20*, 205-208, 1993.
- Shi, G., Global Warming Potential due to chlorofluorocarbons and their substitutes, *Chinese J. Atmos. Sci.*, *16*, 240-248, 1992.
- Shine, K.P., On the cause of the relative greenhouse strength of gases such as the halocarbons, *J. Atmos. Sci.*, *48*, 1513-1518, 1991.
- Shine, K.P., The greenhouse effect and stratospheric change, in *The Role of the Stratosphere in Global Change*, edited by M.-L. Chanin, NATO ASI Series, Springer-Verlag, Berlin, 285-300, 1993.
- Shine, K.P., B.P. Briegleb, A.S. Grossman, D. Hauglustaine, H. Mao, V. Ramaswamy, M.D. Schwarzkopf, R. Van Dorland, and W.-C. Wang, Radiative forcing due to changes in ozone – A comparison of different codes, in *Atmospheric Ozone as a Climate Gas*, edited by W.-C. Wang and I.S.A. Isaksen, NATO ASI Series, Springer-Verlag, Berlin, in press, 1994.
- Slingo A., and H.M. Schrecker, On the shortwave properties of stratiform water clouds, *Quart. J. Roy. Meteorol. Soc.*, *108*, 407-426, 1982.
- Spencer, R.W., and J.R. Christy, Precision lower stratospheric temperature monitoring with the MSU: Validation and results 1979-1991, *J. Climate*, *6*, 1194-1204, 1993.
- Stordal, F., B. Innset, A.S. Grossman, and G. Myhre, SF₆ as a greenhouse gas, *Norwegian Institute for Air Research (NILU) Report 0-92102*, 1993.
- Wallington, T.J., C.A. Gierczak, J.C. Ball, S.M. Japar, Fourier transform infrared study of the self reaction of C₂H₅O₂ radicals in air at 295 K, *Int. J. Chem. Kinet.*, *21*, 1077-1089, 1989.
- Wang, W.-C., J.P. Pinto, and Y.L. Yung, Climatic effects due to halogenated compounds in the Earth's atmosphere, *J. Atmos. Sci.*, *37*, 333-338, 1980.
- Wang W.-C., G.Y. Shi, and J.T. Kiehl, Incorporation of the thermal radiative effect of CH₄, N₂O, CF₂Cl₂ and CFC₁₃ into the NCAR Community Climate Model, *J. Geophys. Res.*, *96*, 9097-9103, 1991.

RADIATIVE FORCING

- Wang, W.-C., Y.-C. Zhuang, and R.D. Bojkov, Climate implications of observed changes in ozone vertical distributions at middle and high latitudes of the Northern Hemisphere, *Geophys. Res. Lett.*, 20, 1567-1570, 1993.
- Wigley, T.M.L., The contribution from emissions of different gases to the enhanced greenhouse effect, in *Climate Change and the Agenda for Research*, edited by T. Hanisch, Westview Press, Boulder, Colorado, 1994.
- WMO, *Atmospheric Ozone, 1985: Assessment of Our Understanding of the Processes Controlling Its Present Distribution and Change*, World Meteorological Organization Global Ozone Research and Monitoring Project – Report No. 16, Geneva, 1986.
- WMO, *Report of the International Ozone Trends Panel*, World Meteorological Organization Global Ozone Research and Monitoring Project – Report No. 18, Geneva, 1988.
- WMO, *Scientific Assessment of Ozone Depletion: 1991*, World Meteorological Organization Global Ozone Research and Monitoring Project – Report No. 25, Geneva, 1992.